

sults. The actual quantitative differences between the two results may be due to differences in rare earth spin matrix elements and to structural variations between the hosts.

¹M. T. Hutchings and W. P. Wolf, Phys. Rev. Letters **11**, 187 (1963).

²W. P. Wolf, M. Ball, M. T. Hutchings, M. J. M. Leask, and A. F. G. Wyatt, J. Phys. Soc. Japan **17**,

Suppl. B-1, 443 (1962).

³R. Orbach, Proc. Roy. Soc. (London), **A264**, 458 (1961).

⁴S. Geschwind, Phys. Rev. **121**, 363 (1961).

⁵Bierig, Weber, and Warschaw (to be published).

⁶T. Moriya, Phys. Rev. **120**, 91 (1960).

⁷S. Geller and M. A. Gilleo, J. Phys. Chem. Solids **3**, 30 (1957).

⁸K. A. Wickersheim, in *Magnetism*, edited by G. T. Rado and H. Suhl, (Academic Press, New York, 1963), Vol. 1, p. 269.

MODE COMPETITION AND COMBINATION TONES IN A GAS LASER

J. Haisma and G. Bouwhuis

Philips Research Laboratories, N. V. Philips' Gloeilampenfabrieken, Eindhoven, The Netherlands

(Received 10 February 1964)

This Letter presents the results of an investigation on the occurrence and on the behavior of a few laser modes of various order with equal frequency spacing during tuning of the laser over half a wavelength.

The laser line is the $2s_2 - 2p_4$ Ne transition (Paschen notation) with a wavelength of 1.153 microns, with a Doppler width at half-maximum intensity of 800 Mc/sec and with an estimated natural linewidth of about 30 Mc/sec at the working pressure.

The measurements were carried out on a short gas laser, described elsewhere,¹ with a mirror separation $L = 12$ cm, giving a longitudinal mode separation of 1250 Mc/sec. Thermal expansion of the laser² shows a periodic series of far-field patterns, apparently corresponding to modes

whose L/λ value is an increasing function, although this increase is not necessarily monotonic.

However, such a simple tuning experiment does not reveal the exact values of frequency and intensity of these modes; each of the observed far-field patterns is in fact a superposition of more than one. Therefore it seemed of interest to us to determine these frequencies. To this end an optical method was used, not only giving exactly the relative frequency values, but simultaneously displaying the corresponding far-field patterns (see Fig. 5 of de Lang and Bouwhuis³). Figure 1 shows schematically the arrangement. As an optical analyzer a one-meter confocal interferometer is used, with a measured "finesse" of 150, corresponding to an instrumental broadening of 0.5 Mc/sec and a resolving power of 6×10^8 at

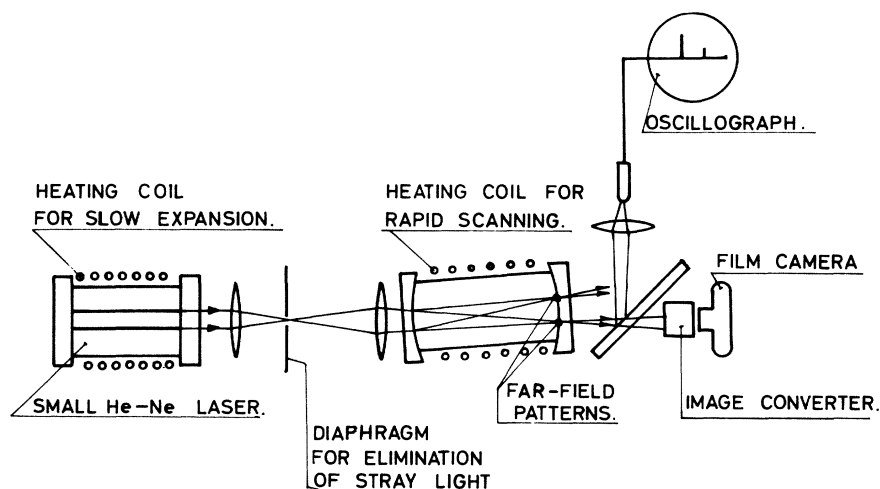


FIG. 1. Experimental arrangement of the optical frequency analysis.

1.15 microns. Apart from ease of adjustment, such a confocal interferometer has the advantage of a highly constant path length for off-axis rays.⁴ This results in an angular field of view which is extremely large as compared to that of the ordinary Fabry-Perot interferometer with flat mirrors, or nonconfocal arrangements with spherical mirrors.⁵ This offers us the possibility to combine the analyzing properties with imaging properties by simply imaging the far-field patterns at the rear interferometer mirror. Rapid scanning of the spectrum is easily achieved by thermal expansion of the interferometer, with oscillographic recording of the transmitted radiation.

As the frequency determination of a Fabry-Perot interferometer is not quite unambiguous, the results were checked by beat measurements. The intensity distribution of the far-field patterns is recorded simultaneously by a film camera via an image converter. The evolution of the spectrum thus recorded was studied as a function of laser length (by slow, thermal expansion of the laser body). The result is given in Fig. 2(a) which shows simultaneously occurring far-field patterns with their frequencies at various laser lengths. The intensities of these various modes, as derived from the peak height of the oscillograms, are plotted in Fig. 2(b) as a function of

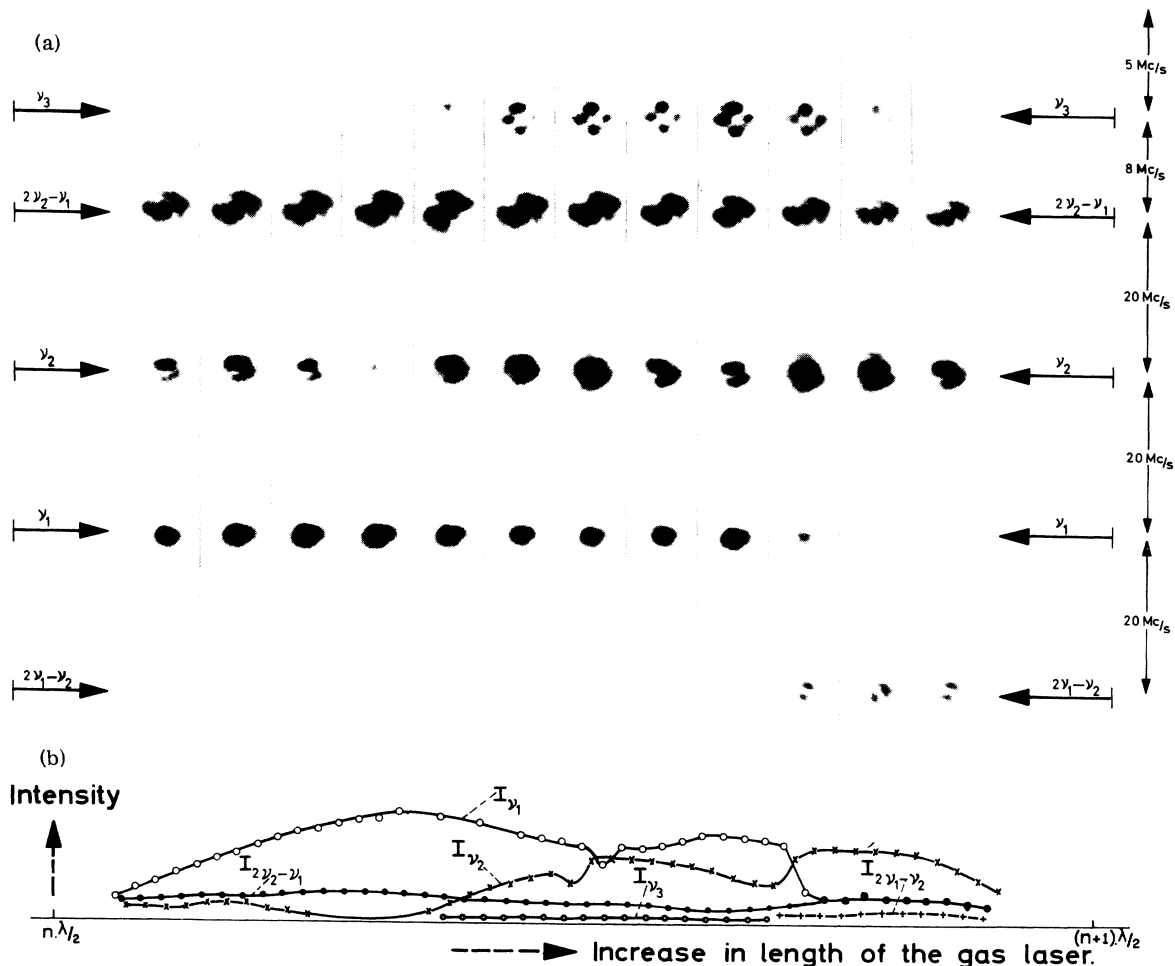


FIG. 2. (a) Far-field patterns as transmitted through the scanning interferometer: from left to right as a function of laser length corresponding to (b); from bottom to top the consecutive transmittance of the scanning interferometer; every column corresponds to tuning over half a wavelength of the scanning interferometer. The quoted values of the frequencies must be corrected due to the frequency shift of the laser line itself during the tuning time of the interferometer over half a wavelength. This correction has been omitted, since we are only interested in relative values, but beat measurements indicate a frequency difference of 12.5 Mc/sec. (b) Intensity of the various modes as a function of laser length.

laser length. The principal modes which occur are the three modes of lowest angular order, TEM_{00} , TEM_{10} , and TEM_{20} (see Fox and Li⁶ for this notation), the intensities of which are denoted by I_{ν_1} , I_{ν_2} , and I_{ν_3} , respectively.

We notice that the increase and decrease of I_{ν_1} and I_{ν_2} is opposite. Moreover, in the center of Fig. 2 both intensities reveal a dip caused by hole-burning effect and the width of this dip indicates a natural linewidth of about 30 Mc/sec. Very remarkable is the transition of the dominant mode intensity on the right-hand side of Fig. 2. We suspect this is due to an asymmetry in the Doppler profile owing to isotope effect.⁷ We intend to check this point with the aid of pure isotopes. The frequency difference between modes ν_1 and ν_2 is smaller than the natural linewidth of the Ne transition. Thus the intensity of both modes arises from the same part of the velocity distribution of the atoms. Besides this the two modes show a spatial overlap as can be seen from Fig. 2(a). These two properties account for the competition between I_{ν_1} and I_{ν_2} during tuning of the gas laser over half a wavelength.

In Fig. 2(a) one observes the expected modes TEM_{00} , TEM_{10} , and TEM_{20} . Curiously, however, between ν_2 and ν_3 there occurs a signal with a frequency equal to $2\nu_2 - \nu_1$ and with an intensity indicated by $I_{2\nu_2 - \nu_1}$ in Fig. 2(b). The intensity distribution of the far-field pattern of this secondary beam looks like a combination of the modes ν_1 and ν_2 . Further, we observe in the lower part of Fig. 2(a) a mode pattern with a similar intensity distribution but with a frequency equal to $2\nu_1 - \nu_2$; its intensity is indicated as $I_{2\nu_1 - \nu_2}$.

The occurrence of these two secondary modes might be explained in any one of the following

three ways:

(1) The patterns are obtained by rapid pulsations between the two principal modes at frequencies ν_1 and ν_2 . Two modes having a frequency spacing smaller than the natural linewidth may cause an amplitude modulation with a frequency equal to the difference frequency of the two "fundamentals."⁸ However, the sequence in frequency of the observed patterns is not in accordance with what one would expect in this case; see Fig. 3.

(2) Both patterns reflect complicated higher order modes, which occur independently of the existence of the fundamental modes. In this case the almost exactly equal frequency spacings (accuracy 20 kc/sec; this value has been obtained by beat measurements) between $2\nu_1 - \nu_2$, ν_1 , ν_2 , and $2\nu_2 - \nu_1$ appear difficult to explain.

(3) The secondary signals are combination tones of the type predicted by Lamb.⁸ A combination tone can arise because of the nonlinear properties of the medium (third-order polarization of the atoms). The surprisingly large intensity of the combination tones could presumably be due to the amplifying properties of this medium at these frequencies together with the resonant character of the combination tone in the laser. The fact that one of the "fundamental" modes apparently disappears, and the combination tone does not, is indeed remarkable. However, some remanent intensity may still be present, and the competition between the combination tone and its nearest "fundamental" neighbor in frequency might now produce the large intensity difference. This would mean that the behavior of such a combination tone is not determined by the third-order polarization only, but to a large extent by the properties of the multiresonant system.

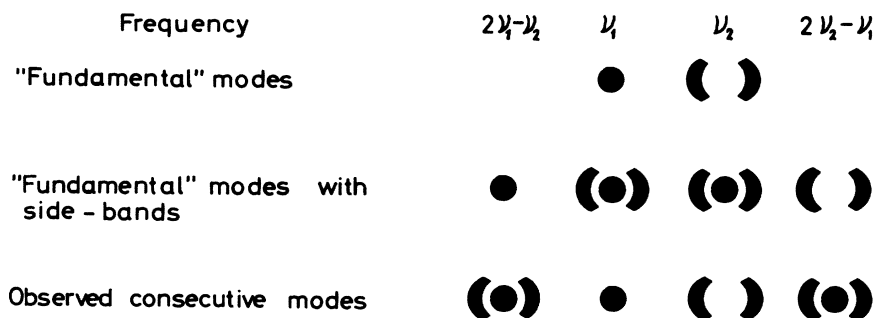


FIG. 3. Plot (schematic) of consecutive modes when pulsations of the "fundamentals" play a role. Below, the observed sequence of the modes.

We ourselves prefer this third explanation. However, more evidence of a quantitative nature is needed to support this suggestion.

We greatly appreciate the stimulating discussions with Dr. H. de Lang and Professor H. G. van Bueren.

¹H. G. van Bueren, J. Haisma, and H. de Lang, Phys. Letters 2, 340 (1962).

²J. Haisma and H. de Lang, Phys. Letters 3, 240 (1963).

³H. de Lang and G. Bouwhuis, Phys. Letters 5, 48

(1963).

⁴P. Connes, J. Phys. Radium 19, 262 (1958).

⁵D. R. Herriott, Appl. Opt. 2, 865 (1963).

⁶A. G. Fox and T. Li, Bell System Tech. J. 40, 453 (1961).

⁷A. Szöke and A. Javan, Phys. Rev. Letters 10, 521 (1963).

⁸W. E. Lamb, Jr., Proceedings of the Third International Symposium on Quantum Electronics, Paris, February 1963 (to be published); Proceedings of the Scuola Internazionale di Fisica "Enrico Fermi" on Quantum Electronics and Coherent Light, Varenna, Italy, August 1963 (unpublished).

ANGULAR DEPENDENCE OF MASER-STIMULATED RAMAN RADIATION IN CALCITE*

R. Chiao and B. P. Stoicheff[†]

Massachusetts Institute of Technology, Cambridge, Massachusetts

(Received 14 February 1964)

One of the most striking characteristics of maser-stimulated Raman scattering is the specific directional emission of the Stokes and anti-Stokes radiation.^{1,2} Here, we report on experimental studies of this angular dependence in calcite. We have observed four orders of anti-Stokes emission in well-defined cones, diffuse first-order Stokes emission with cones of absorption in this diffuse radiation, and a well-defined cone of second-order Stokes emission, all in the forward direction. Since the refractive index of calcite is precisely known,³ it has been possible to predict accurately these maxima and minima of anti-Stokes and Stokes radiation on the basis of the following wave vector relations:

$$\vec{k}_0 + \vec{k}_{n-1} = \vec{k}_{-1} + \vec{k}_n, \quad (1)$$

$$\vec{k}_0 + \vec{k}_{-1} = \vec{k}_{n-1} + \vec{k}_{-n}, \quad (1')$$

where \vec{k}_0 , \vec{k}_{-1} , \vec{k}_n , and \vec{k}_{-n} are, respectively, the maser, the first Stokes, and the n th-order anti-Stokes and Stokes waves vectors. From these observations it is concluded that in our experiments on the stimulated Raman scattering in calcite, the dominant process is that proposed by Garmire, Pandarese, and Townes.⁴

According to their theory, diffuse first-order Stokes radiation (of frequency $\omega_0 - \omega_r$) is initially produced by the very intense maser light (ω_0), and subsequently anti-Stokes and Stokes radiation of many orders ($\omega_0 \pm n\omega_r$) is produced by the interaction of the maser light with the first-order Stokes radiation. These higher order Raman effects proceed according to the wave vector re-

lations (1) and (1') for three-dimensional interactions, and should give rise to absorption of first-order Stokes radiation and to emission of anti-Stokes and higher order Stokes radiation in cones around the maser beam. The theoretical values for the angles of the n th-order anti-Stokes emission from (1) are given by

$$\theta_n = \beta_n \pm (\beta_n^2 + \delta_n - \gamma_n)^{1/2}, \quad (2)$$

where

$$\beta_n = k_{n-1} \theta_{n-1} / (k_{-1} + k_n),$$

$$\delta_n = 2(k_{-1}/k_n)(k_n + k_{-1} - k_0 - k_{n-1}) / (k_{-1} + k_n),$$

$$\gamma_n = (k_{n-1} - k_{-1}) \beta_n \theta_{n-1} / k_r.$$

The corresponding angles of first-order Stokes absorption are

$$\theta_{-1}^{(n)} = (k_{n-1} \theta_{n-1} - k_n \theta_n) / k_{-1}. \quad (3)$$

Equations (2) and (3) also give the angles of the n th-order Stokes emission and corresponding first-order Stokes absorption when \vec{k}_n is replaced by $-\vec{k}_{-n}$ and \vec{k}_0 by $-\vec{k}_0$.

In our experiments, a calcite crystal 5 to 10 cm long was placed in the path of the focused external beam from a giant pulse ruby maser (with rotating prism). The maser output power was in excess of 10 megawatts in a 30-nsec pulse. The crystal was oriented so that the maser beam, which was linearly polarized, traveled through the crystal as the ordinary ray. In this orienta-

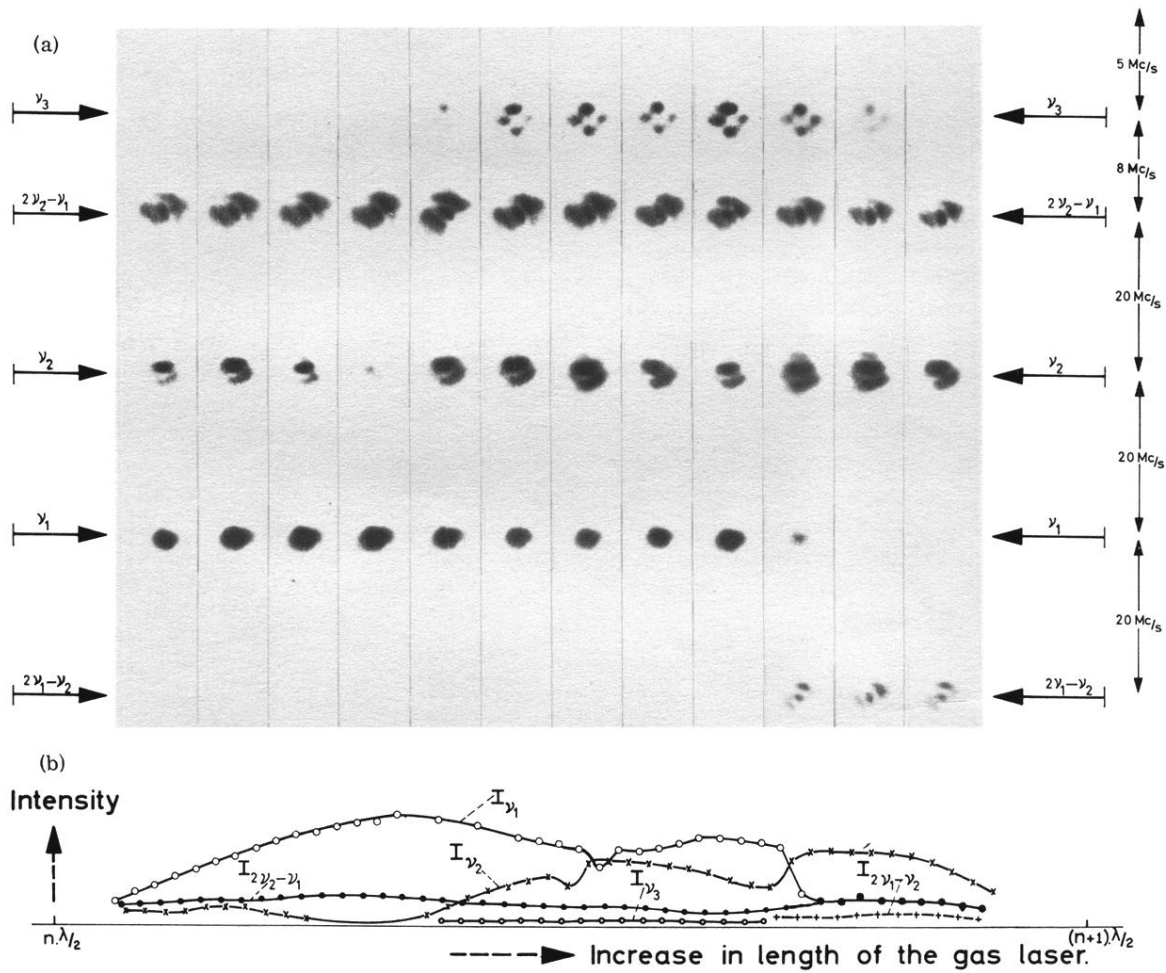


FIG. 2. (a) Far-field patterns as transmitted through the scanning interferometer: from left to right as a function of laser length corresponding to (b); from bottom to top the consecutive transmittance of the scanning interferometer; every column corresponds to tuning over half a wavelength of the scanning interferometer. The quoted values of the frequencies must be corrected due to the frequency shift of the laser line itself during the tuning time of the interferometer over half a wavelength. This correction has been omitted, since we are only interested in relative values, but beat measurements indicate a frequency difference of 12.5 Mc/sec. (b) Intensity of the various modes as a function of laser length.